Received: 13 July 2021 | Accepted: 21 August 2021

DOI: 10.1111/srt.13106

ORIGINAL ARTICLE

WILEY

Vasomotion analysis of speed resolved perfusion, oxygen saturation, red blood cell tissue fraction, and vessel diameter: Novel microvascular perspectives

Ingemar Fredriksson[1] | Marcus Larsson[1] | Tomas Strömberg[1] | Fredrik Iredahl[2,3]

[1] Department of Biomedical Engineering, Linköping University, Linköping, Sweden

[2] Department of Health, Medicine and Caring Sciences, Linköping UniversityDivision of Community Medicine, Linköping, Sweden

[3] Department of Primary health care, Region Östergötland, Linköping, Sweden

Correspondence
Fredrik Iredahl, Åby vårdcentral, Nyköpingsvägen 28, 61630 Åby, Sweden.
Email: fredrik.iredahl@liu.se

Abstract

Background: Vasomotion is the spontaneous oscillation in vascular tone in the microcirculation and is believed to be a physiological mechanism facilitating the transport of blood gases and nutrients to and from tissues. So far, Laser Doppler flowmetry has constituted the gold standard for in vivo vasomotion analysis.

Materials and methods: We applied vasomotion analysis to speed-resolved perfusion, oxygen saturation, red blood cell tissue (RBC) tissue fraction, and average vessel diameter from five healthy individuals at rest measured by the newly developed Periflux 6000 EPOS system over 10 minutes. Magnitude scalogram and the time-averaged wavelet spectra were divided into frequency intervals reflecting endothelial, neurogenic, myogenic, respiratory, and cardiac function.

Results: Recurrent high-intensity periods of the myogenic, neurogenic, and endothelial frequency intervals were found. The neurogenic activity was considerably more pronounced for the oxygen saturation, RBC tissue fraction, and vessel diameter signals, than for the perfusion signals. In a correlation analysis we found that changes in perfusion in the myogenic, neurogenic, and endothelial frequency intervals precede changes in the other signals. Furthermore, changes in average vessel diameter were in general negatively correlated to the other signals in the same frequency intervals, indicating the importance of capillary recruitment.

Conclusion: We conclude that vasomotion can be observed in signals reflecting speed resolved perfusion, oxygen saturation, RBC tissue fraction, and vessel diameter. The new parameters enable new aspects of the microcirculation to be observed.

KEYWORDS
diffuse reflectance spectroscopy, laser Doppler flowmetry, microcirculation, vasomotion

1 | INTRODUCTION

Vasomotion is the spontaneous oscillation in vascular tone in the microcirculation and is believed to be a physiological mechanism facilitating the transport of blood gases and nutrients to and from tissues. Vasomotion can be described as recurrent organized fluctuations in vessel diameter notable over time. By frequency analysis, distinct frequency intervals related to physiological aspects can be presented as heart rate, respiration, myogenic activity, neurogenic, and endothelial dependent activity.[1] The higher frequency intervals that can be verified by measurement of pulse and respiration frequency are related to cardiac and pulmonary pressure variation. The myogenic interval has been studied in animal models and by mapping of cellular mechanisms.[2–4] The neurogenic interval has been studied by blockage of sympathetic nerves using microdialysis catheters delivering bretylium tosylate.[5] The endothelial interval has been studied by iontophoresis of the acetylcholine, an endothelium-dependent vasodilator, and sodium nitroprusside, an endothelium independent vasodilator,[6] and by inhibition of endothelial nitric oxide synthase by intradermal microdialysis leading to suppression of the endothelial interval.[7]

Vasomotion analysis potentially offers measures that are more directly related to physiological mechanisms than the measurement of microvascular perfusion alone and have been utilized to investigate microvascular dysfunction in various disease states. Type 2 diabetes is a well-known risk factor for microvascular dysfunctions including neuropathy.[8] Alterations in the neurogenic frequency has been observed in patients with type 2 diabetes[9,10–12] and type 1 diabetes.[13] Vasomotion has also been used to study altered microvascular endothelial function during smoking,[14] benign and malignant melanocytic skin lesions and has been found to be a specific, sensitive method for the in vivo identification of malignant melanoma,[15] in patients with paranoid schizophrenia,[16] schizophrenia,[17] lepromatous leprosy patients,[18] obesity,[19] systemic sclerosis patients,[20] alcoholic withdrawal syndrome,[21] venous insufficiency,[22] during general anesthesia[23] and compared between different ages[5] as well as been used in description of pharmacological properties of drugs such as exenatide.[24] Although studied in many patient groups, it has still not reached clinical routine.

Laser Doppler flowmetry (LDF) has constituted the gold standard for in vivo vasomotion analysis. Other methods used have been photoplethysmography,[25] correlation mapping optical coherence tomography (cmOCT),[26] and high-precision ultrasonic echotracking device.[27] The Periflux 6000 EPOS system (Perimed AB, Järfälla, Stockholm, Sweden) combines LDF and diffuse reflectance spectroscopy (DRS) to assess speed resolved perfusion, red blood cell (RBC) tissue fraction, oxygen saturation, and average microvascular vessel diameter, simultaneously from the same measurement volume.[28,29] The related instrument O2C (Lea Medizintechnik, Giessen, Germany) combines the assessment of conventional (not speed-resolved) perfusion, relative blood concentration, and oxygen saturation in a similar manner. These techniques enable further analysis of the physiological aspects involved in vasomotion. Since vasomotion appears from smooth muscle vasodilation and vasoconstriction resulting in variation of vessel lumen and recruitment of capillaries, the Periflux 6000 EPOS that enables assessment of the vessel diameter is hypothesized to be suitable for vasomotion analysis.

Different authors have used different techniques to calculate the frequency intervals. The most commonly used method for analyzing vasomotion has been the wavelet transformation,[30,31] followed by the short-time Fourier transform.[32,33] A multitude of different normalization strategies have also been used, regarding normalization of the signals prior to the transformation calculations, and normalization of the energy in the studied frequency bands. Furthermore, the borders of the frequency intervals vary slightly between authors. The lack of consensus regarding the analysis of vasomotion patterns makes it difficult to compare results between studies. Therefore, a methodological standardization is needed to facilitate future comparisons and reach clinical application.

The aim of this study was to present a framework for vasomotion analysis of signals related to oxygen saturation, RBC tissue fraction, average vessel diameter, and speed resolved perfusion. We analyzed the data using scalograms of individual signals and by correlation between the signals, enabling a deeper understanding of local microvascular regulation.

2 | MATERIAL AND METHODS

2.1 | Measurement system

Data were recorded using the Periflux 6000 EPOS system (Perimed AB, Järfälla-Stockholm, Sweden).[28,34,35] The system collects both DRS and LDF data from the same tissue volume. The data analysis is based on artificial neural networks that has been trained on modeled data with added system specific noise, using measured spectra as input and any of the output parameters oxygen saturation, RBC tissue fraction, average vessel diameter, speed resolved perfusion, or sample depth as output.[36] In the case of speed-resolved perfusion, both DRS and LDF spectra were used as input, whereas only the DRS spectra were used in the other cases.

Normally, the average vessel diameter is not an output from the EPOS system. However, the shape of the DRS spectra are affected in a characteristic manner when the average vessel diameter is changed, due to the so called vessel packaging effect,[37,38] and we have previously shown that this effect can be used to estimate the average vessel diameter from DRS spectra.[28,39]

The sample depth was estimated based on the depths of the photon paths. The sample depth was defined as the depth above which $1 - \exp(-1) \approx 63\%$ of the photon paths were situated. The photon paths and thus this sample depth were known in the training data, and a separate artificial neural network was trained to the sample depth. Also compare with the sampling volume description in Fredriksson et al.[28]

Data were collected at 15 Hz sampling frequency, that is, 15 sets of spectra per second.

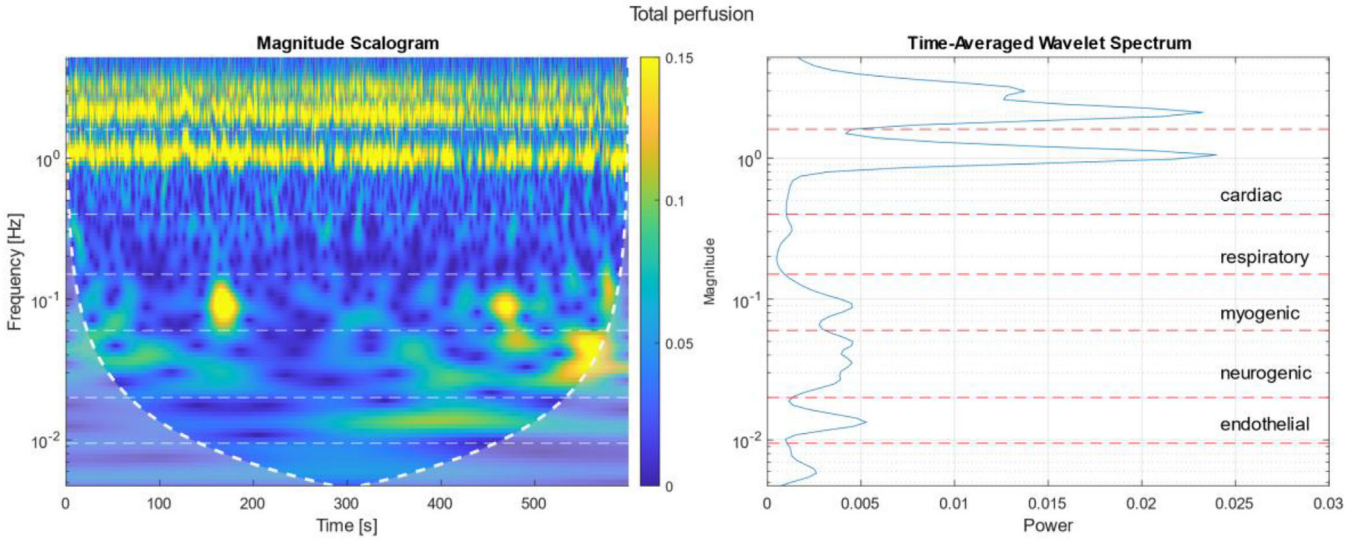

FIGURE 1 Example of magnitude scalogram and the time-averaged wavelet spectrum for total perfusion. The frequency limits between the five different frequency intervals are marked with the dashed lines. Overtones of the heart frequency (sligtly above 1 Hz) at about 2 and 4 Hz can be observed

2.2 | In vivo measurements

Data were collected on five healthy volunteers (two females) aged 21–42 years, BMI 19–28 kg/m^2, without regular medication and no known skin disease. The subjects gave their written informed consent before the start of the measurement, and the protocol was approved by the Swedish Ethical Review Authority, d.no. 2019–04713. The measurement probe was attached using double-adhesive tape (PF 105-1, Perimed AB) on the volar side of the right forearm, about 15 cm above the wrist, avoiding any visible vessels. Before the start of the measurement, the subjects rested for 20 min in the same room and in the same position as data later was recorded. After acclimatization, each subject was recorded during a period of 10 min. The room temperature was measured during the experiment and kept within the range of 21–22°C.

2.3 | Wavelet analysis

The oscillations in the measured microvascular signals caused by vasomotion as well as respiration and heart beats have period lengths varying from about 1 s (heartbeat) to more than a minute. In this study, the frequency content is analyzed using the Morlet wavelet transformation.[30,31] Similar results can be obtained by using the short-time Fourier transform.[32,33] An advantage with the wavelet analysis is that the time resolution is different for different frequencies, partially overcoming the problem to choose between high time resolution or high frequency resolution. Another advantage is that the frequency resolution can be adapted to a logarithmic frequency scale, which is advantageous for visual representation.

The conventional perfusion signal was normalized with its mean value before the wavelet calculation. From a theoretical fluid mechanics perspective, this normalization adds to two important effects. Firstly, it makes the signals insensitive to the overall perfusion in the sampling volume, and secondly, it makes the signals sensitive to relative variations in vessel diameter. All speed-resolved perfusion signals as well as the total perfusion (sum of the speed-resolved perfusion) were normalized with the average total perfusion for the same reason. The RBC tissue fraction signal was normalized with its mean, and the wavelet was calculated from the square-root of the normalized signal, since it can be argued that variation in the square-root is related to variations in the vessel diameter. For the oxygen saturation and the vessel diameter signals, no normalization was done.

All signals were further pre-processed by subtracting the mean to avoid spectral leakage from the zero frequency. For the signals that were normalized, the subtraction of the mean was done after normalization.

The Morlet wavelet transform was calculated by using the Wavelet Toolbox in Matlab 2021a (The MathWorks, Inc). The calculation results in a scalogram that is a 2D-map of signal magnitude to scale and time, where the scale corresponds to the frequency, sometimes denoted pseudo-frequency. A time-averaged power spectrum was calculated as the time average of the squared scalogram for each frequency. An example is seen in Figure 1. The shaded area in the magnitude spectrogram at low frequencies denotes times where the border effect significantly affects the estimation of the magnitude for those frequencies. Those areas have been excluded when calculating the time-averaged wavelet spectrum.

The magnitude scalogram and the time-averaged wavelet spectrum were divided into the following frequency intervals: endothelial 0.0095–0.02 Hz, neurogenic 0.02–0.06 Hz, myogenic 0.06–0.15 Hz, respiratory 0.15–0.4 Hz, and cardiac 0.4–1.6 Hz. These intervals are identical to the once used by Stefanovska, Bracic et al,[30] and similar to those used by for example Söderström, Stefanovska et al,[40] Humeau, Koïtka et al,[31] and Rossi, Bazzichi et al.[20]

2.4 | Correlation analysis

In addition to the wavelet analysis, the covariation between the different signals in the different frequency intervals was also analyzed. This was done by first applying zero-phase band-pass filtering with a fourth order Butterworth filter with the frequency limits of each of the five frequency intervals given above. Then, the cross-correlation between each pair of signals, for example between total perfusion and oxygen saturation in the endothelial frequency interval, was calculated. The time-shift corresponding to the maximum absolute correlation, limited to $\pm 1(3f_{high})$ where f_{high} is the upper cut-off frequency of the given frequency interval, was considered. An analysis by the maximum correlation and the time shift that corresponds to, reveals information about potential synchronization in the physiological processes underlying the different microvascular signals.

3 | RESULTS

The estimated sample depth was 0.4 mm in the measurements from all five test subjects.

3.1 | Examples from one individual

In Figures 2–5, example magnitude scalograms and time-averaged wavelet spectra are shown for one of the five subjects. For the speed resolved perfusion, speeds < 1 and > 1 mm/s are chosen, as well as the total perfusion. For comparison with previous works, results for conventional perfusion are also shown, and these are very similar to the results for total perfusion.

There are several differences and similarities in the patterns of the different types of signals. Comparing perfusion for speeds below and above 1 mm/s, respectively, reveals that the frequencies related to cardiac activity is more pronounced for the higher speed region, which is generally the case for all five test subjects. Furthermore, the energy for speeds > 1 mm/s is much higher than for the low speeds indicating that the perfusion variations are larger for higher speeds. It can also be seen that the peaks in the myogenic and neurogenic intervals are more visible in relation to the other frequency intervals for the lower speed, but that is not a general trend for all five test subjects.

The cardiac and respiratory frequency intervals are considerably less pronounced for the non-perfusion signals, that is, oxygen saturation, RBC tissue fraction, and vessel diameter. They are almost indiscernible for the oxygen saturation. That is the case for all five subjects.

The general pattern of the magnitude scalograms of the high-intensity periods of the myogenic, neurogenic, and endothelial frequency intervals is similar in all signals. One example is the high intensity region at about 200 s in the myogenic frequency interval, that is clearly visible in all signals. But there are also differences in how they are pronounced for the different signals. For example, in general for all five test persons, especially the neurogenic activity is considerably more pronounced in relation to the total energy for the oxygen saturation, RBC tissue fraction, and vessel diameter signals, than for the perfusion signals. That can be seen when comparing the neurogenic frequency interval in the time-averaged wavelet spectra in Figure 2, with the corresponding interval in Figures 3–5. In the latter case, there is a clear peak, whereas that is hardly discernible in the spectra from the perfusion signals.

Another interesting aspect to notice in the magnitude scalograms is the long time between periods of high activity. Studying Figure 5, in the myogenic frequency interval, these periods appear with intervals of 100–200 s, whereas in the neurogenic frequency interval, there is only one such high-activity period.

3.2 | Summarized results for all test subjects

In Table 1, the average (standard deviation) of the total energy in each frequency interval for each signal, including conventional (conv.) perfusion, is given. The averages and standard deviations are calculated for the five subjects. The total energy is calculated from the time-averaged wavelet spectra.

3.3 | Correlation between signals

Results of the correlation analysis for the neurogenic frequency interval (0.02–0.06 Hz) are shown in Tables 2–4. We have chosen to include time shifts only for absolute correlation coefficients exceeding a threshold of 0.5, since the estimation of the time shift is less accurate for smaller correlation coefficients. That also emphasizes the cases when the absolute correlation coefficient is high. It can be seen that the absolute correlation coefficient is above 0.5 in the majority of the test subjects for correlations between: total perfusion and oxygen saturation; total perfusion and vessel diameter; and oxygen saturation and vessel diameter. In all cases where the correlation coefficient exceeded 0.5, the time shift between the total perfusion and the other signals was negative, meaning that the change in the total perfusion preceded the change in the other signal (oxygen saturation, RBC tissue fraction, and vessel diameter). Estimated time shifts between oxygen saturation and RBC tissue fraction, oxygen saturation and vessel diameter, and RBC tissue fraction and vessel diameter were much smaller.

It can be observed that the vessel diameter is generally negatively correlated with the other signals. That is true for all cases where the absolute correlation coefficient exceeds 0.5, also for the frequency intervals not shown in Tables 2–4. The correlation between all other signals is positive where the absolute correlation coefficient is above 0.5.

In Table 5, number of subjects having an absolute maximum correlation coefficient exceeding 0.5 between the different signals in the three lowest frequency intervals, it is summarized how many of the five test subjects that had a maximum absolute correlation coefficient above 0.5 for correlations between the different signals for the myogenic, neurogenic, and endothelial frequency intervals. For the respiratory and cardiac frequency intervals, there were no absolute

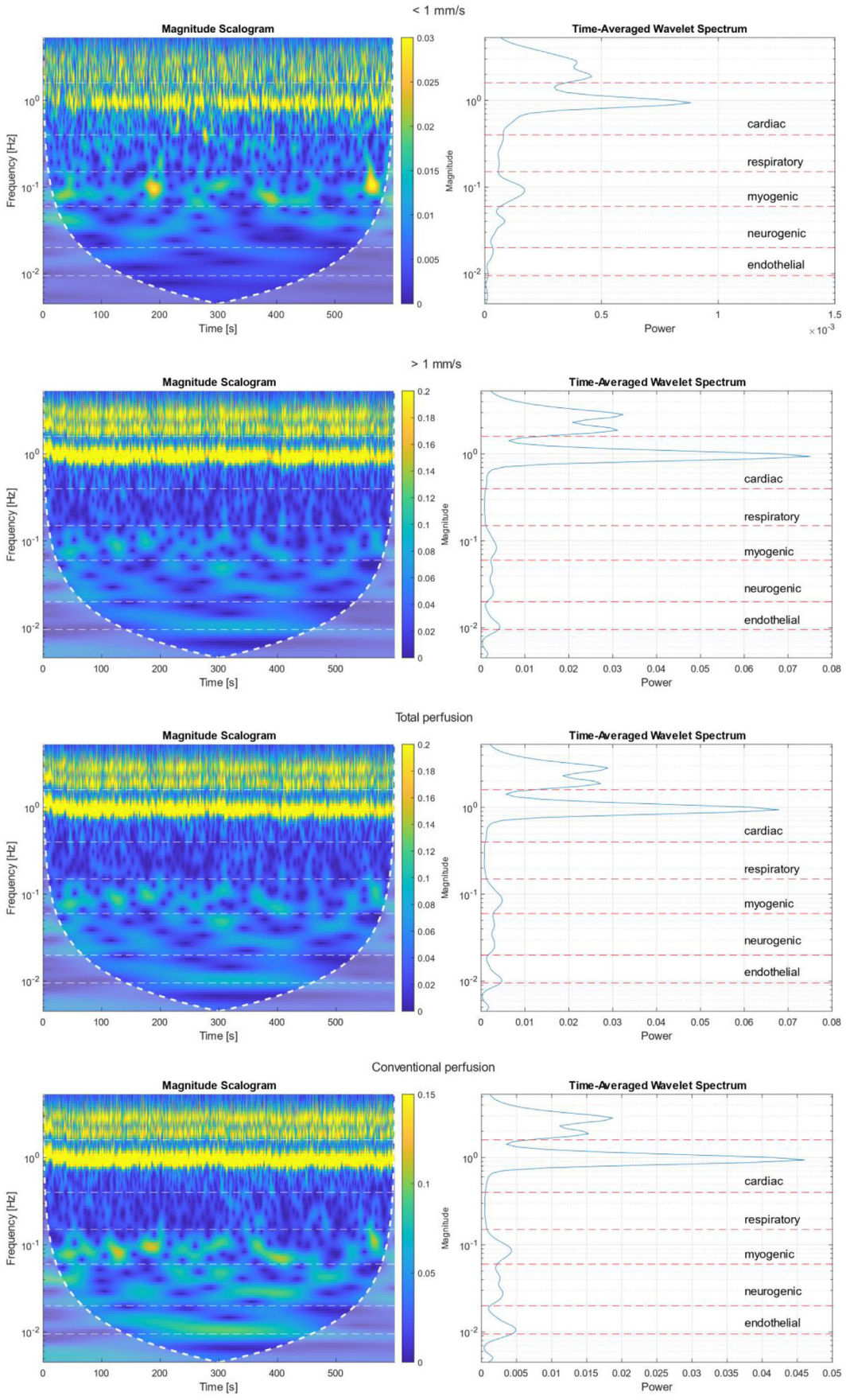

FIGURE 2 Magnitude scalograms and time-averaged wavelet spectra for speed resolved and conventional perfusion

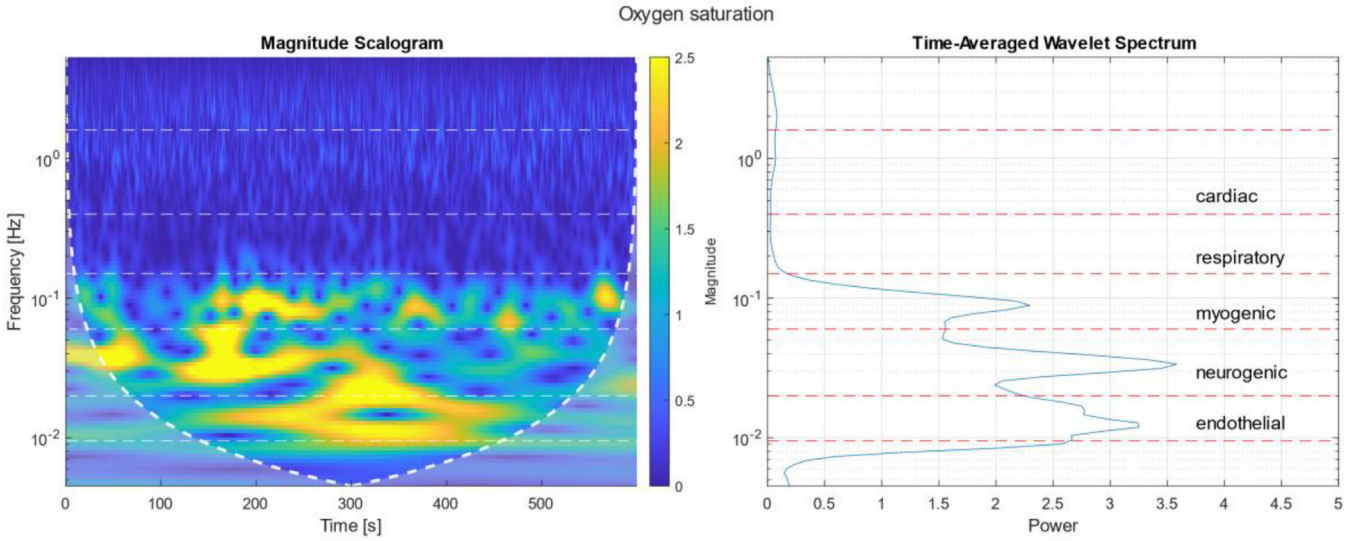

FIGURE 3 Magnitude scalograms and time-averaged wavelet spectra for oxygen saturation

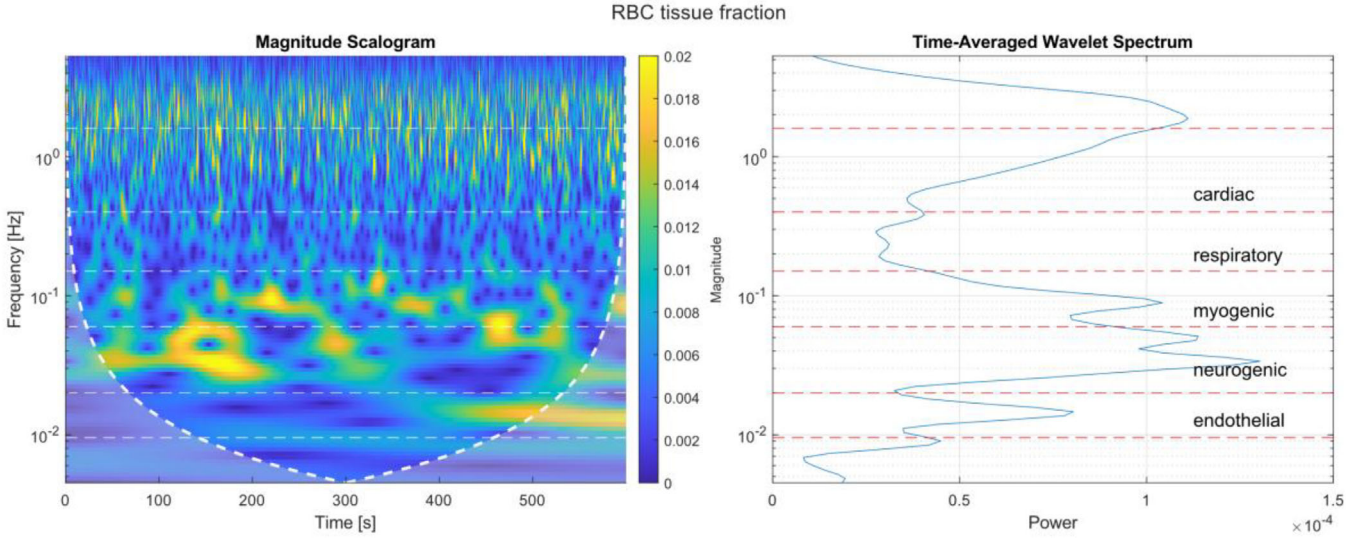

FIGURE 4 Magnitude scalograms and time-averaged wavelet spectra for RBC tissue fraction

correlation coefficients exceeding 0.5 between: perfusion and oxygen saturation; perfusion and RBC tissue fraction; perfusion and vessel diameter; oxygen saturation and vessel diameter; or RBC tissue fraction and vessel diameter. For the cardiac frequency interval, there was a (weak) negative correlation between oxygen saturation and RBC tissue fraction, between −0.3 and −0.6 for all five test subjects.

The correlation coefficient between perfusion for speeds below 1 mm/s and total perfusion was above 0.5 in all cases for the endothelial, neurogenic, and myogenic frequency intervals, but below 0.5 in most cases for the respiratory and cardiac frequency interval. The situation was similar for the correlation of perfusion for speeds below 1 mm/s to above 1 mm/s. The correlation coefficient between perfusion for speeds above 1 mm/s and total perfusion was above 0.5 in all cases for all frequency intervals. The correlation between perfusion and oxygen saturation, RBC tissue fraction, and average vessel diameter was in all cases similar no matter if total perfusion or only perfusion below or above 1 mm/s was considered. Therefore, we choose to present such results only for the total perfusion and not for the perfusion divided into low or high speeds.

An example of the correlation between total perfusion and oxygen saturation is shown in Figure 6, and an example between oxygen saturation and vessel diameter is shown in Figure 7.

4 | DISCUSSION

We have introduced new signals possible for vasomotion analysis enabling new tools to investigate the microcirculation. The oxygen saturation and vessel diameter signals represent dimensions of the microcirculation that are intuitively relatively independent from the

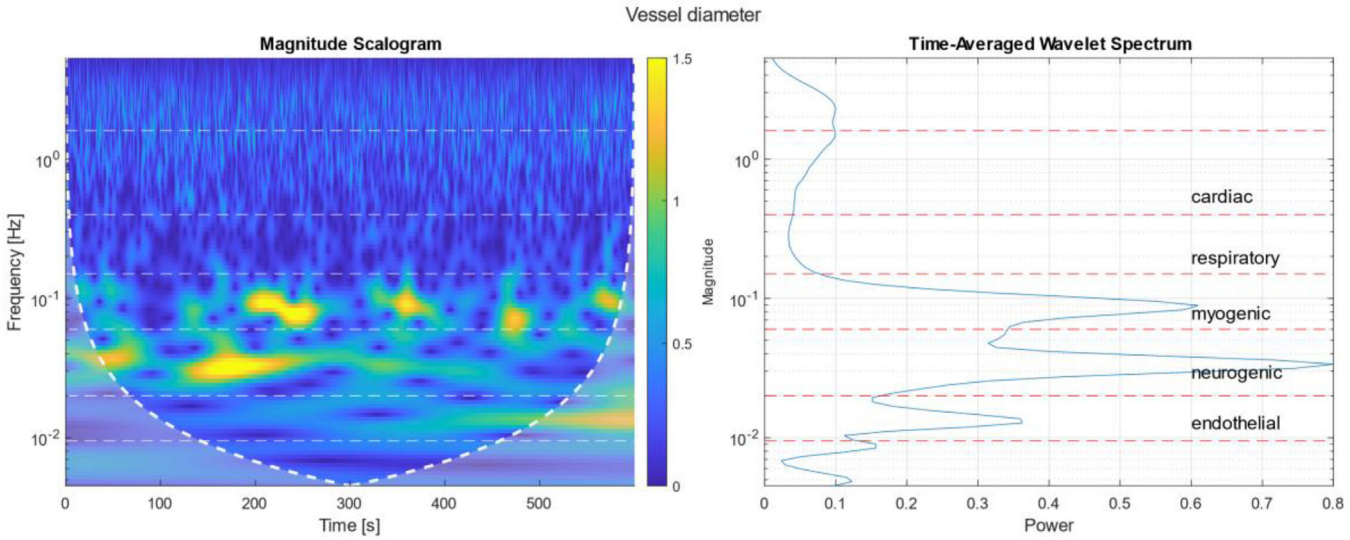

FIGURE 5 Magnitude scalograms and time-averaged wavelet spectra for average vessel diameter

TABLE 1 Total energy in each frequency interval. Data presented as mean (standard deviation) over the five test subjects

	Perfusion						
Frequency interval	<1 mm/s				Oxygen saturation	RBC tissue fraction	Vessel diameter
Cardiac 0.4–1.6 Hz	0.016 (0.014)	0.20 (0.13)	0.22 (0.16)	0.14 (0.10)	0.63 (0.26)	0.00074 (0.00036)	1.2 (0.2)
Respiratory 0.15–0.4 Hz	0.0036 (0.0039)	0.0039 (0.055)	0.053 (0.083)	0.031 (0.041)	0.39 (0.22)	0.00026 (0.00013)	0.62 (0.39)
Myogenic 0.06–0.15 Hz	0.0026 (0.0019)	0.029 (0.020)	0.042 (0.030)	0.032 (0.018)	6.7 (7.1)	0.00040 (0.00037)	1.5 (1.8)
Neurogenic 0.02–0.06 Hz	0.0027 (0.0017)	0.031 (0.012)	0.045 (0.012)	0.042 (0.015)	25 (15)	0.00083 (0.00064)	3.5 (2.6)
Endothelial 0.0095–0.02 Hz	0.0010 (0.0006)	0.014 (0.010)	0.020 (0.011)	0.021 (0.013)	16 (10)	0.00047 (0.00017)	1.6 (0.8)

perfusion. That is manifested by the much less impact of the cardiac and respiratory frequency intervals on those signals. Even if not clearly seen in the data presented in this study, it is also possible that the vasomotion analysis of the perfusion signals originating from blood flow with different speeds can lead to new insights in the underlying physiology of vasomotion, not seen with conventional perfusion. Vasomotion based on conventional perfusion has to date been by far the most common choice, now challenged by these new signals.

Vasomotion can be described as recurrent fluctuations in vessel diameter, and the introduction of the vessel diameter signal is a more direct observation than the conventional perfusion signal. It has been suggested that the oscillatory pattern leads to a more favorable tissue perfusion and oxygenation.[41] Negative correlation between average vessel diameter and total perfusion, oxygen saturation and RBC fraction, was generally observed in this study. The variation in the average vessel diameter signal could either be explained by variation in vessel diameter in each active vessel, or in combination with a local

TABLE 2 Maximum correlation coefficient and time shift for the maximum correlation coefficient when it exceeded 0.5 between total perfusion and oxygen saturation, RBC tissue fraction, and vessel diameter, respectively, for the neurogenic frequency interval

	Oxygen		RBC tissue fraction		Vessel diameter	
Subject	Time shift	Correlation coefficient	Time shift	Correlation coefficient	Time shift	Correlation coefficient
1		0.19		0.12		0.38
2	−4.7	0.72		0.37	−3.7	−0.57
3		0.40		−0.19		0.35
4	−2.5	0.62	−1.0	0.54	−1.5	−0.52
5	−4.4	0.80	−2.9	0.68	−4.6	−0.66

TABLE 3 Same as Table 2 but correlation between oxygen saturation and RBC tissue fraction and vessel diameter, respectively

	RBC tissue fraction		Vessel diameter	
Subject	Time shift	Correlation coefficient	Time shift	Correlation coefficient
1		0.37		−0.49
2		0.19	1.3	−0.80
3		0.20	−1.3	−0.54
4	1.2	0.61	0.8	−0.87
5	−0.1	0.73	0.4	−0.88

TABLE 4 Same as Table 2 but correlation between RBC tissue fraction and vessel diameter

	Vessel diameter	
Subject	Time shift	Correlation coefficient
1		−0.40
2		0.08
3		0.42
4	−0.5	−0.62
5	0.9	−0.60

capillary recruitment explained by the theory where the lowering of resistance in terminal arterioles increase the perfusion of nutritive capillary beds.[42] Capillary recruitment would lead to a smaller average vessel diameter. Increased capillary recruitment would inherently increase RBC fraction and also oxygen saturation in the case of constant metabolism. Thus, negative correlation indicates that variation in the average vessel diameter signal foremost depends on capillary recruitment, and not diameter changes in individual vessels. The sample depth of in the measurements was 0.4 mm, likely foremost including capillary, arteriole, and venule blood vessels with limited smooth muscle control.

Speed resolved perfusion and optically assessed average vessel diameter has for the first time been used in the analysis of vasomotion. Vasomotion has previously been observed in signals related to oxygen saturation[43] and RBCs have been proposed as a sensor of local tissue hypoxia.[44] RBC tissue fraction can be compared with photoplethysmography that has previously been used to asses vasomotion.[25]

The origin of the cardiac and pulmonary frequency interval is based on central pressure variation. Although frequency analysis can identify these parameters, they should not be misinterpreted with local regulations of the myogenic, neurogenic, and endothelial intervals.

Traditionally, vasomotion has been measured for 5–30 min. Based on the scalograms in Section 3.1, the chosen 10 min protocol in this study may have been too short to accurately estimate the energy within the lower frequency intervals. Possibly is vasomotion a tool for precision medicine, and we recommend future studies to observe over a longer-time period as well in larger cohorts. To our knowledge, observations of vasomotion over significantly longer time have not been studied.

In this study, we have used the Morlet wavelet transform to calculate vasomotion energy in various frequency intervals. Principally equal results could have been achieved using the Fourier transform, but the wavelet transform was preferred for better visualization of the scalograms. The normalization strategy has a larger impact on the results when comparing different subjects. We have chosen to normalize some of the signals (perfusion and RBC tissue fraction) so that the vasomotion energy in those signals depends on relative variations and not on the mean signal value. We argue that this normalization results in energies that reflect the relative variation in vessel diameter more accurately, than analyzing unnormalized perfusion. For the oxygen saturation and vessel diameter signals, the same argumentation does not apply, and thus we choose not to use normalization for those signals. Furthermore, we do not perform a normalization of the energy in the various frequency intervals to the total energy for all frequencies, as was for example proposed in,[30,40] as such normalization introduces a constructed correlation between the various frequency bands which we think is unwanted. The normalization with the mean of the signal, as done for example for the perfusion signals, has the same effect as was probably intended with the normalization with the total energy, without causing such unwanted correlations.

Based on the small number of study subjects, any conclusion related to standard deviation should be handled with caution, but we see rather large variations within this group of healthy subjects. The microcirculation is sensitive for factors such as temperature, and therefore we chose a period of 20 min acclimatization and a temperature-controlled room to standardize the measurements. Spatial and/or temporal heterogeneity could be another explanation to the observed variations between individuals. Spatial variations have previously been observed by single point measuring techniques[43,45] with possible individual difference. Recently established spatial measurement techniques, such as Laser Speckle Contrast Imaging, could constitute a tool to further elucidate the potential spatial variations. Another limitation is the lack of provocation to emphasize the endothelial frequency component. Since vasomotion needs relatively long observational periods to limit the effect of temporal variation, heating could be a suitable provocation. Different aspects of vasomotion may be emphasized by different provocations such as local heating[33] or physical activity where the local metabolism and oxygen consumption is changed.

We observed a time shift between increased local perfusion followed by increased oxygenation. It has previously been proposed that vasomotion is a mechanism regulating local oxygen supply where an oxygen saturation below a certain threshold triggers increased perfusion, that in turn increases the oxygen saturation.[44,46] That would explain this time shift. Differences have been observed between lean and obese subjects,[44] but this mechanism has so far not been studied in patients with known microvascular dysfunction.

Standardization of vasomotion analysis would facilitate comparisons between different studies. However, the introduction of new parameters leading to increased understanding of physiological

TABLE 5 Number of subjects having an absolute maximum correlation coefficient exceeding 0.5 between the different signals in the three lowest frequency intervals

	Vessel diameter			RBC tissue fraction			Oxygen saturation		
	Endothelial	Neurogenic	Myogenic	Endothelial	Neurogenic	Myogenic	Endothelial	Neurogenic	Myogenic
Total perfusion	1	3	1	0	2	0	3	3	2
Oxygen saturation	4	4	5	3	2	1			
RBC tissue fraction	3	2	1						

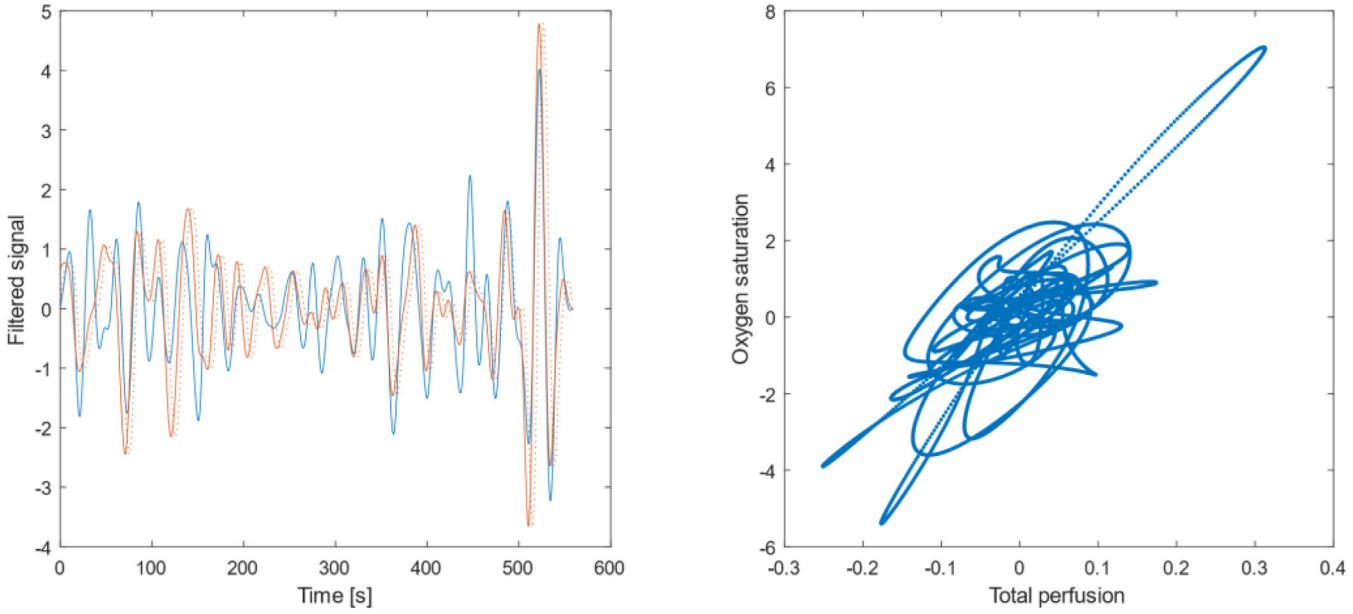

FIGURE 6 Total perfusion (blue curve) and oxygen saturation (red curve) as a function of time after band-pass filtering with cut-off frequencies 0.02 and 0.06 Hz, and normalization with their respective standard deviation to facilitate comparison (A). The oxygen saturation signal with no time-shift is represented by the dotted red curve. In (B), the two signals are plotted against each other, where changes are generally found along the positive diagonal giving a positive correlation

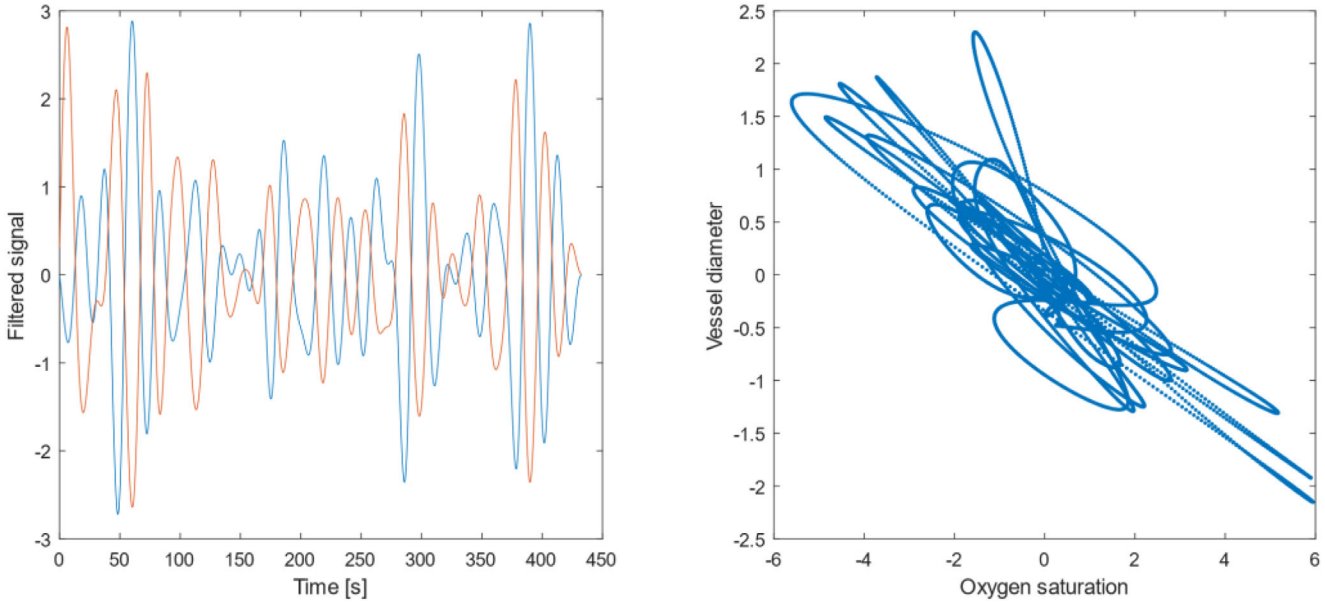

FIGURE 7 Oxygen saturation (blue curve) and average vessel diameter (red curve) as a function of time after band-pass filtering with cut-off frequencies 0.02 and 0.06 Hz, and normalization with their respective standard deviation to facilitate comparison (A). In (B), the two signals are plotted against each other, where changes are generally found along the negative diagonal giving a negative correlation. The estimated time-shift giving the maximum correlation was negligible and not included in these plots

mechanism highlights the need of new interpretation models before such standardization can take place. In addition, future studies will reveal how to make best use of the information found when combining the different microvascular signals. Is there for example clinically important information about the metabolism that can be revealed by a simultaneous analysis of the vasomotion of the speed-resolved perfusion and oxygen saturation signals?

A noninvasive instrument that objectively detects microvascular dysfunction before clinical complications appear would have a natural place within preventive care of patients with for example type 2 diabetes. Oxygen signal analysis in patients with known affected lung function would also be of interest, such as in lung fibrosis and chronic obstructive pulmonary disease.

5 | CONCLUSION

Vasomotion can be observed in signals reflecting speed resolved perfusion, oxygen saturation, RBC tissue fraction, and vessel diameter. The vasomotion analysis reveals similarities and potentially important differences between the signals, enabling new aspects of the microcirculation to be observed such as underlying mechanisms for capillary recruitment.

ACKNOWLEDGMENTS

The authors would like to acknowledge Dr. Robin Mirdell for valuable assistance during data acquisition.

CONFLICT OF INTEREST

Dr. Fredriksson is part-time employed by Perimed AB, which is developing products related to research described in this publication. All other authors declare that there is no conflict of interest that could be perceived as prejudicing the impartiality of the research reported.

ORCID

Ingemar Fredriksson https://orcid.org/0000-0002-3454-6576
Marcus Larsson https://orcid.org/0000-0001-6385-6760
Tomas Strömberg https://orcid.org/0000-0002-7299-891X
Fredrik Iredahl https://orcid.org/0000-0002-4245-7565

REFERENCES

1. Cracowski J-L, Roustit M. Human skin microcirculation. Compr Physiol;2020;10:1105–54.
2. Colantuoni A, Bertuglia S, Intaglietta M. Quantitation of rhythmic diameter changes in arterial microcirculation. Am J Physiol. 1984;246(4 Pt 2):H508–17.
3. Meyer JU, Borgström P, Lindbom L, Intaglietta M. Vasomotion patterns in skeletal muscle arterioles during changes in arterial pressure. Microvasc Res. 1988;35(2):193–203.
4. Aalkjaer C, Nilsson H. Vasomotion: cellular background for the oscillator and for the synchronization of smooth muscle cells. Br J Pharmacol. 2005;144(5):605–16.
5. Hodges GJ, Mallette MM, Martin ZT, Del Pozzi AT. Effect of sympathetic nerve blockade on low-frequency oscillations of forearm and leg skin blood flow in healthy humans. Microcirculation. 2017;24(7):e12388.
6. Kvernmo HD, Stefanovska A, Kirkeboen KA, Kvernebo K. Oscillations in the human cutaneous blood perfusion signal modified by endothelium-dependent and endothelium-independent vasodilators. Microvasc Res. 1999;57(3):298–309.
7. Stewart JM, Taneja I, Goligorsky MS, Medow MS. Noninvasive measure of microvascular nitric oxide function in humans using very low-frequency cutaneous laser Doppler flow spectra. Microcirculation. 2007;14(3):169–80.
8. Chatterjee S, Khunti K, Davies MJ. Type 2 diabetes. Lancet. 2017;389(10085):2239–51.
9. Bernardi L, Rossi M, Leuzzi S, Mevio E, Fornasari G, Calciati A, et al. Reduction of 0.1 Hz microcirculatory fluctuations as evidence of sympathetic dysfunction in insulin-dependent diabetes. Cardiovasc Res. 1997;34(1):185–91.
10. Sun PC, Chen CS, Kuo CD, Lin HD, Chan RC, Kao MJ et al. Impaired microvascular flow motion in subclinical diabetic feet with sudomotor dysfunction. Microvasc Res. 2012;83(2):243–8.
11. Sun PC, Kuo CD, Chi LY, Lin HD, Wei SH, Chen CS. Microcirculatory vasomotor changes are associated with severity of peripheral neuropathy in patients with type 2 diabetes. Diab Vasc Dis Res. 2013;10(3):270–6.
12. Schiappacassa A, Maranhão PA, Souza M, Panazzolo DG, Nogueira Neto JF, Bouskela E, et al. Acute effects of metformin and vildagliptin after a lipid-rich meal on postprandial microvascular reactivity in patients with type 2 diabetes and obesity: a randomized trial. J Clin Med. 2020;9(10):3228.
13. Sorelli M, Francia P, Bocchi L, De Bellis A, Anichini R. Assessment of cutaneous microcirculation by laser Doppler flowmetry in type 1 diabetes. Microvasc Res. 2019;124:91–6.
14. Rossi M, Pistelli F, Pesce M, Aquilini F, Franzoni F, Santoro G, et al. Impact of long-term exposure to cigarette smoking on skin microvascular function. Microvasc Res. 2014;93:46–51.
15. Häfner HM, Bräuer K, Eichner M, Steins A, Möhrle M, Blum A, et al. Wavelet analysis of cutaneous blood flow in melanocytic skin lesions. J Vasc Res. 2005;42(1):38–46.
16. Israel AK, Seeck A, Boettger MK, Rachow T, Berger S, Voss A, et al. Peripheral endothelial dysfunction in patients suffering from acute schizophrenia: a potential marker for cardiovascular morbidity? Schizophr Res. 2011;128(1-3):44–50.
17. Voss A, Seeck A, Israel A-K, Bär K-J. Enhanced spectral analysis of blood flow during post-occlusive reactive hyperaemia test in different tissue depths. Auton Neurosci. 2013;178(1):15–23.
18. Treu C, de Souza M, Lupi O, Sicuro FL, Maranhão PA, Kraemer-Aguiar LG, et al. Structural and functional changes in the microcirculation of lepromatous leprosy patients - Observation using orthogonal polarization spectral imaging and laser Doppler flowmetry iontophoresis. PLoS One. 2017;12(4):e0175743.
19. Jonk AM, Houben AJ, Schaper NC, de Leeuw PW, Serné EH, Smulders YM, et al. Meal-related increases in microvascular vasomotion are impaired in obese individuals: a potential mechanism in the pathogenesis of obesity-related insulin resistance. Diabetes Care. 2011;34(Suppl 2):S342–48.
20. Rossi M, Bazzichi L, Di Maria C, Franzoni F, Raimo K, Della Rossa A, et al. Blunted increase of digital skin vasomotion following acetylcholine and sodium nitroprusside iontophoresis in systemic sclerosis patients. Rheumatology (Oxford). 2008;47(7):1012–17.
21. Jochum T, Weissenfels M, Seeck A, Schulz S, Boettger MK, Voss A, et al. Endothelial dysfunction during acute alcohol withdrawal syndrome. Drug Alcohol Depend. 2011;119(1-2):113–22.
22. Heising S, Haase H, Sippel K, Riedel F, Jünger M. Cutaneous vasomotion in patients with chronic venous insufficiency and the influence of compression therapy. Clin Hemorheol Microcirc. 2009;41(1):57–66.

23. Landsverk SA, Kvandal P, Bernjak A, Stefanovska A, Kirkeboen KA. The effects of general anesthesia on human skin microcirculation evaluated by wavelet transform. Anesth Analg. 2007;105(4):1012–19.
24. Smits MM, Muskiet MH, Tonneijck L, Kramer MH, Diamant M, van Raalte DH, et al. GLP-1 receptor agonist exenatide increases capillary perfusion independent of nitric oxide in healthy overweight men. Arterioscler Thromb Vasc Biol. 2015;35(6):1538–43.
25. Korhonen I, Yli-Hankala A. Photoplethysmography and nociception. Acta Anaesthesiol Scand. 2009;53(8):975–85.
26. Smirni S, MacDonald MP, Robertson CP, McNamara PM, O'Gorman S, Leahy MJ, et al. Application of cmOCT and continuous wavelet transform analysis to the assessment of skin microcirculation dynamics. J Biomed Opt. 2018;23(7):1–13.
27. Porret CA, Stergiopulos N, Hayoz D, Brunner HR, Meister JJ. Simultaneous ipsilateral and contralateral measurements of vasomotion in conduit arteries of human upper limbs. Am J Physiol. 1995;269(6 Pt 2):H1852–8.
28. Fredriksson I, Burdakov O, Larsson M, Strömberg T. Inverse Monte Carlo in a multilayered tissue model: merging diffuse reflectance spectroscopy and laser Doppler flowmetry. J Biomed Opt. 2013;18(12):127004.
29. Jonasson H, Fredriksson I, Pettersson A, Larsson M, Strömberg T. Oxygen saturation, red blood cell tissue fraction and speed resolved perfusion - A new optical method for microcirculatory assessment. Microvasc Res. 2015;102:70–7.
30. Stefanovska A, Bracic M, Kvernmo HD. Wavelet analysis of oscillations in the peripheral blood circulation measured by laser Doppler technique. IEEE Trans Biomed Eng. 1999;46(10):1230–9.
31. Humeau A, Koïtka A, Abraham P, Saumet J-L, L'Huillier J-P. Spectral components of laser Doppler flowmetry signals recorded in healthy and type 1 diabetic subjects at rest and during a local and progressive cutaneous pressure application: scalogram analyses. Phys Med Biol. 2004;49(17):3957–70.
32. Serné EH, IJzerman RG, Gans ROB, Nijveldt R, de Vries G, Evertz R, et al. Direct evidence for insulin-induced capillary recruitment in skin of healthy subjects during physiological hyperinsulinemia. Diabetes. 2002;51(5):1515–22.
33. Del Pozzi AT, Miller JT, Hodges GJ. The effect of heating rate on the cutaneous vasomotion responses of forearm and leg skin in humans. Microvasc Res. 2016;105:77–84.
34. Fredriksson I, Saager RB, Durkin AJ, Strömberg T. Evaluation of a pointwise microcirculation assessment method using liquid and multilayered tissue simulating phantoms. J Biomed Opt. 2017;22(11):1–9.
35. Jonasson H, Fredriksson I, Larsson M, Strömberg T. Validation of speed-resolved laser Doppler perfusion in a multimodal optical system using a blood-flow phantom. J Biomed Opt. 2019;24(9):1–8.
36. Fredriksson I, Larsson M, Strömberg T. Machine learning for direct oxygen saturation and hemoglobin concentration assessment using diffuse reflectance spectroscopy. J Biomed Opt. 2020;25(11):112905.
37. Svaasand L, Fiskerstrand E, Kopstad G, Norvang L, Svaasand E, Nelson J et al. Therapeutic response during pulsed laser treatment of port-wine stains: Dependence on vessel diameter and depth in dermis. Lasers Med Sci. 1995;10(4):235–43.
38. van Veen RLP, Verkruysse W, Sterenborg HJCM. Diffuse-reflectance spectroscopy from 500 to 1060 nm by correction for inhomogeneously distributed absorbers. Opt Lett. 2002;27(4):246–8.
39. Fredriksson I, Larsson M, Strömberg T. Accuracy of vessel diameter estimated from a vessel packaging compensation in diffuse reflectance spectroscopy. Munich, Germany: SPIE; 2011.
40. Söderström T, Stefanovska A, Veber M, Svensson H. Involvement of sympathetic nerve activity in skin blood flow oscillations in humans. Am J Physiol Heart Circ Physiol. 2003;284(5):H1638–646.
41. Kanick SC, Schneider PA, Klitzman B, Wisniewski NA, Rebrin K. Continuous monitoring of interstitial tissue oxygen using subcutaneous oxygen microsensors: in vivo characterization in healthy volunteers. Microvasc Res. 2019;124:6–18.
42. Clark MG. Impaired microvascular perfusion: a consequence of vascular dysfunction and a potential cause of insulin resistance in muscle. Am J Physiol Endocrinol Metab. 2008;295(4):E732–50.
43. Stücker M, Steinbrügge J, Ihrig C, Hoffmann K, Ihrig D, Röchling A, et al. Rhythmical variations of haemoglobin oxygenation in cutaneous capillaries. Acta Derm Venereol. 1998;78(6):408–11.
44. Thorn CE, Kyte H, Slaff DW, Shore AC. An association between vasomotion and oxygen extraction. Am J Physiol Heart Circ Physiol. 2011;301(2):H442–9.
45. Kano T, Shimoda O, Higashi K, Sadanaga M. Effects of neural blockade and general anesthesia on the laser-Doppler skin blood flow waves recorded from the finger or toe. J Auton Nerv Syst. 1994;48(3):257–66.
46. Thorn CE, Shore AC. The role of perfusion in the oxygen extraction capability of skin and skeletal muscle. Am J Physiol Heart Circ Physiol. 2016;310(10):H1277–84.

How to cite this article: Fredriksson I, Larsson M, Strömberg T, Iredahl F. Vasomotion analysis of speed resolved perfusion, oxygen saturation, red blood cell tissue fraction, and vessel diameter: Novel microvascular perspectives. Skin Res Technol. 2021; 1–11. https://doi.org/10.1111/srt.13106